

# ‘SWEATCH’: A Wearable Platform for Harvesting and Analysing Sweat Sodium Content

Tom Glennon,<sup>[a]</sup> Conor O’Quigley,<sup>[a]</sup> Margaret McCaul,<sup>[a]</sup> Giusy Matzeu,<sup>[a]</sup> Stephen Beirne,<sup>[b]</sup> Gordon G. Wallace,<sup>[b]</sup> Florin Stroeescu,<sup>[c]</sup> Niamh O’Mahoney,<sup>[c]</sup> Paddy White,<sup>[c]</sup> and Dermot Diamond<sup>\*[a]</sup>

**Abstract:** A platform for harvesting and analysing the sodium content of sweat in real time is presented. One is a ‘watch’ format in which the sampling and fluidic system, electrodes, circuitry and battery are arranged vertically, while in the other ‘pod’ format, the electronics and battery components, and the fluidics electrodes are arranged horizontally. The platforms are designed to be securely attached to the skin using a velcro strap. Sweat enters into the device through a sampling orifice and passes over solid-state sodium-selective and reference electrodes and into a storage area containing a high capacity adsorbent material. The liquid movement is entirely driven by capillary action, and the flow rate through the device can be mediated through variation of the width of a fluidic channel linking the electrodes to the sample storage area. Changing the width dimension through 750, 500 and 250  $\mu\text{m}$  produces flow rates of 38.20, 21.48 and 6.61  $\mu\text{L}/\text{min}$ , respectively. Variation of

the sweat uptake rate and the storage volume capacity enables the duration of usage to be varied according to the needs of the user. The devices can be easily disassembled to replace the electrodes and the high capacity adsorbent material. The storage sweat is available for subsequent measurement of the total volume of sweat harvested and the average concentration of sodium over the period of use. Signals generated by the electrodes are passed to a custom designed electronics board with high input impedance to accurately capture the voltage. The real-time data is transmitted wirelessly using incorporated Bluetooth circuitry to a remote basestation (laptop, mobile phone, tablet) for data visualization and storage in standard formats. Results obtained during trials over a period of ca. 30 minutes controlled exercise are consistent with previously published data, showing a gradual relatively slow increase of the sodium concentration in the sweat during this period.

**Keywords:** Sweat • Wearables • Sodium • Ion-Selective Electrode • Hydration

## 1 Introduction

Interest in real-time monitoring of biochemical parameters using wearable/on-body sensors is a rapidly growing area of research [1], due in part to the convergence of interest of major economic sectors in applications based on new types of information. ICT companies like Apple and Google are exploring ways to access biochemical information as a means to move beyond the mature sensor technologies currently employed in exercise and sports APPs that track a users location, body movements, temperature, energy expenditure and so on. These are typically based on physical transducers or imaging technologies embedded within wristbands or smart phones. However, employing similar approaches that depend on time-series data to the domain of biochemical sensing is much more difficult, due to the complex challenges associated with access to representative samples (typically a body fluid) and the less predictable behavior of chemical sensors and biosensors over time.

Since the exciting developments of the 1980’s, the application of biochemical sensing to real-time monitoring of the human condition has scarcely advanced in terms of the performance of the sensors. Today, the use-model has almost entirely shifted away from the early over-optimistic promise of implantable sensors that are in continuous

contact with blood [2], to devices sited outside the body that somehow can access an information rich body fluid, like sweat [3][4] or saliva [5]. For the past several decades, the predominant use model for health related diagnostics has been the disposable single-shot sensor combined with a finger prick access to blood samples. Examples of use models that involve real-time monitoring of body fluids (albeit over relatively short periods typically at most up to several days) include the integration of biosensors with contact lenses that can sample and report on the composition of ocular fluid, which is in turn reflective of the systemic blood composition [6]. Perhaps the best-known example of this is the collaborative venture between Google and Novartis [7], based on Parvis’s work

[a] T. Glennon, C. O’Quigley, M. McCaul, G. Matzeu, D. Diamond  
Insight Centre for Data Analytics, National Centre for Sensor Research, Dublin City University, Dublin 9, Ireland  
\*e-mail: dermot.diamond@dcu.ie

[b] S. Beirne, G. G. Wallace  
ARC Centre of Excellence for Electromaterials Science, University of Wollongong NSW2522, Australia

[c] F. Stroeescu, N. O’Mahoney, P. White  
Shimmer, DCU Innovation Campus, Glasnevin, Dublin 11, Ireland

on glucose sensing [6]. Printable, conformable biosensors have recently been integrated onto the contact lens platform, and the use model is attractive in that the lens is disposable, typically being replaced on a daily basis [8]. Biochemical sensors have also been employed on skin, either through physical attachment such that the sensors access sweat induced by exercise or iontophoresis [9], or interstitial fluid accessed through the skin using micro-needles [10]. The recently published sweat-band that can track the wearer's temperature, glucose, lactate, potassium and sodium from exercise induced sweat appears to be a significant advance [11]. The Abbott 'Libre' interstitial glucose sensor can be attached to the shoulder or other body locations using a customized applicator that simultaneously punctures the skin to access interstitial fluid. The device can be left in position for up to 2 weeks according to the specifications [12]. The group of Rogers has been particularly active in the development of conformable printable electronics and sensors that are produced in a tattoo format that can be transferred to the skin [13]. For a recent overview of non-invasive electrochemical wearable sensors see the review by Bandodkar and Wang [14].

As in all analytical methods, access to a representative sample is vital. With biochemical on-body sensing this is compounded by difficulties associated with the need for invasive sampling through the skin to access blood or interstitial fluid. Sweat and ocular fluid are particularly attractive analytical media as access is non-invasive. Sweat is obtained either through exercise or induced locally using techniques like pilocarpine iontophoresis. Important applications for sweat analysis relate to monitoring of personal hydration status for athletes and persons exposed to extreme conditions [15] and for certain clinical

conditions like cystic fibrosis, in which the normal range of electrolyte composition of sweat becomes significantly unbalanced. Monitoring of sweat electrolytes could also play an important role in qualifying the efficacy of new therapeutic treatments for conditions like Cystic Fibrosis, as these are typically designed to restore the normal intra- and extra-cellular electrolyte balance, which in turn should be manifested as a return to more normal sodium levels in sweat [14].

In this paper, we present two platforms designed to harvest and analyse sweat continuously as it emerges through the skin. Data generated is accessible remotely using via wireless Bluetooth connectivity.

## 2 Experimental

### 2.1 Platform Design

The sweat-monitoring platform is designed to allow close, direct skin contact for sweat sampling while protecting the individual device components within a custom-designed enclosure. Two platform designs have been investigated, a 'watch' type design in which the electronics and fluidics components are arranged vertically (Fig. 1a), and a 'pod' like design in which the electronics and fluidics components are arranged horizontally in separate compartments (Fig. 1b). Each platform incorporates a miniaturized wireless data logging circuit protected by a 3D printed dual polymer casing. The main body of the casing is produced using the rigid polymer VEROWHITEPLUS RGD835. This is printed simultaneously with the softer polymer TANGOBLACKPLUS FLX980 (both from Stratasys, UK) to provide flexibility and sealing between the assembled components. The components include

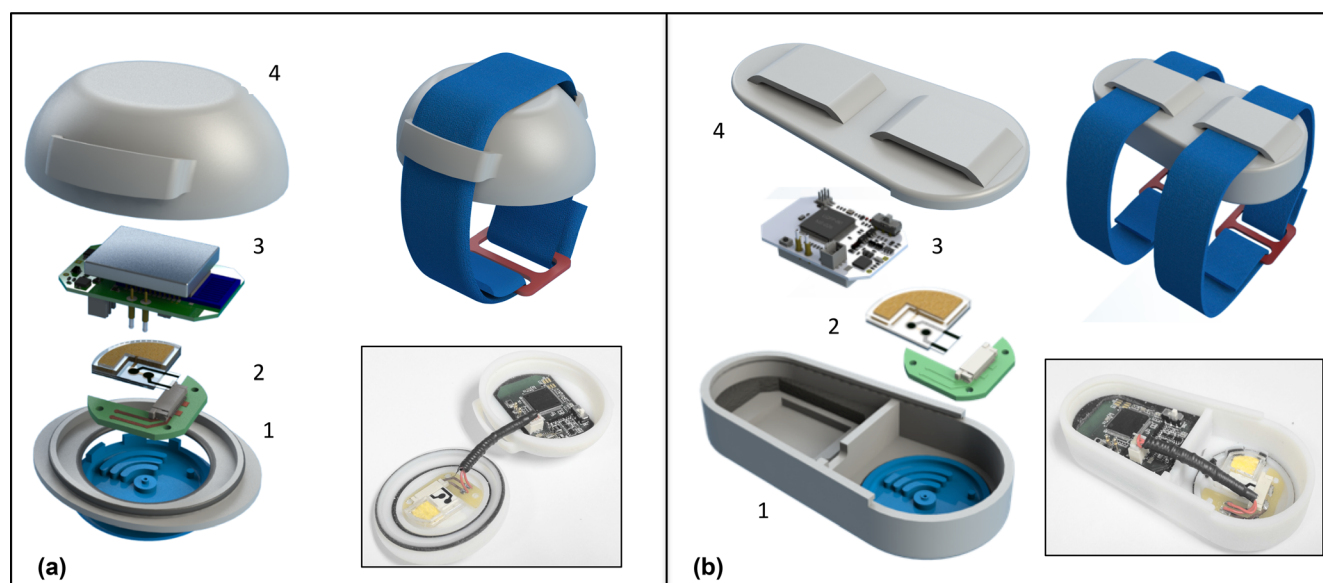


Fig. 1. "Watch" type (a) with vertical arrangement and "Pod" type platform (b) with horizontal arrangement of electronics and fluidics components consisting of 1: sweat harvesting device in 3d-printed platform base, 2: fluidic sensing chip, 3: electronic data logger and battery, and 4: 3d-printed upper casing.

a sweat harvesting base plate with a centrally located sweat entry point, screen-printed ion-selective (ISE) and reference (RE) electrodes, incorporated in a microfluidic chip for  $\text{Na}^+$  sensing, an electronic board for data logging and wireless communications (Shimmer), and a rechargeable lithium battery. The Shimmer board is custom designed, and includes high impedance inputs to ensure the ISE potentials are tracked accurately.

## 2.2 Materials

The carbon and dielectric inks used in the preparation of the screen-printed electrodes were obtained from Gwent Inc. Pontypool, UK (product codes C2030519P4 and D50706D2, respectively). PET sheets (175  $\mu\text{m}$  thick HiFi, Dublin, Ireland) were used as the electrode substrate, while pressure-sensitive adhesive (86  $\mu\text{m}$ , PSA-AR9808, Adhesives Research, Ireland) and PMMA (0.5 mm, 1.5 mm and 3.0 mm thick) was obtained from GoodFellow, UK. Highly absorbent material (Superior Cleanroom Products <http://superiorcleanroomproducts.com/index.html>, product number 87109), was used to generate spontaneous fluid movement through the platform by capillary action, assisted by placement of cotton threads in the channel (removed from medical bandages, W.O.W. Bandage BP, 5 cm  $\times$  5 cm).

Sodium chloride, 3,4-ethylenedioxythiophene (EDOT, 97%), high molecular weight poly(vinyl chloride) (PVC), tetrahydrofuran (THF,  $\geq 99.5\%$ ), 4-*tert*-butylcalix[4]arene-tetraacetic acid tetraethyl ester (sodium ionophore X), potassium tetrakis(4-chlorophenyl)borate (KTFPB), bis(2-ethylhexyl)sebacate, 2,2-dimethoxy-2-phenylacetophenone (DMPA,  $>99\%$ ), butyl-acrylate ( $>99\%$ ) and 1,6-hexanediol diacrylate (HDDA, 80%), all selectophore grade, where available, were purchased from Sigma-Aldrich (Dublin, Ireland). *N*-Decyl-methacrylate was obtained from Polysciences (Northampton, UK). 1-Ethyl-3-methylimidazolium bis(trifluoromethanesulfonyl)imide [emim][NTf<sub>2</sub>], [emim] tris(pentafluoroethyl)trifluorophosphate [FAP] and 1-hexyl-3-methylimidazolium [hmim][FAP] were obtained from VWR (Dublin, Ireland). All chemicals were used without any further purification. Milli-Q reagent-grade deionised water (resistivity 18.2 M $\Omega$  cm) was used for making all aqueous solutions.

## 2.3 Electrochemical Sensors

The solid-state ISE (based on the calix[4]arene tetraester  $\text{Na}^+$  ionophore X [17]), and RE were prepared on a conducting carbon ink insulated by a dielectric layer. These layers were screen printed using a DEK 248 printer on 175  $\mu\text{m}$  thick PET sheets using the protocol previously reported by Zuliani et al. [18].

There are many strategies for creating solid state ISEs and REs which have been reviewed recently [19]. In this study, a poly-3,4-ethylenedioxythiophene (PEDOT) solid contact layer was electrodeposited on the exposed carbon layers using 3,4-ethylenedioxythiophene (EDOT, 97%,

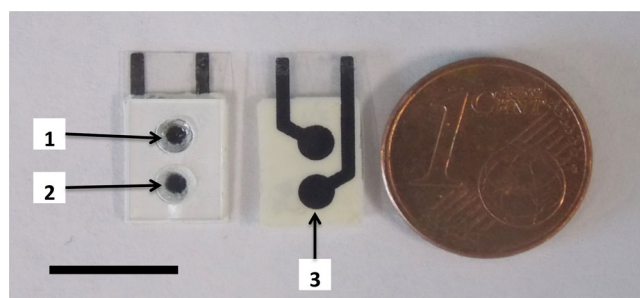


Fig. 2. Front (left) and back (right) of the electrochemical sensor showing (1) the ISE, (2) the reference electrode and (3) the screen printed conductive carbon layer. Scale bar = 1 cm

483028 Aldrich) and [emim] tris-(pentafluoroethyl)trifluorophosphate [FAP] (VWR, Dublin, Ireland) as this approach had been previously demonstrated to produce electrodes with excellent characteristics. [20] Two separate 3.0 mm diameter reservoirs were laser cut in 500  $\mu\text{m}$  PMMA. The ISE and reference polymer membranes were prepared in these by drop casting (see below) and attached to the screen-printed layers using 86  $\mu\text{m}$  pressure sensitive adhesive (PSA), from Adhesives Research, Ireland (Fig. 2).

For the  $\text{Na}^+$  ISE a total of 30  $\mu\text{L}$   $\text{Na}^+$  selective membrane material dissolved in THF was drop-cast into the reservoir above the solid-contact PEDOT layer in the following sequence: 2.5  $\mu\text{L}$  (once); 3  $\mu\text{L}$  (5 times); 2.5  $\mu\text{L}$  (once); 2  $\mu\text{L}$  (twice); 1.5  $\mu\text{L}$  (twice) and 1  $\mu\text{L}$  (3 times) in order to build up polymer layers to fill the 3.5  $\mu\text{L}$  reservoir. We have found that this sequence of additions produces electrodes with good quality sealing between the electrode cover layer and the substrate layer, while also enabling the PVC membrane to be built up gradually to fill the reservoir volume. For the reference membrane, a cocktail was prepared of ionic liquid (IL) vortexed for 1 h with the acrylate monomer(s), the cross-linker and the photoinitiator. This was then photopolymerised within the 3 mm reservoir by irradiation for 32 minutes with a CL-1000 ultraviolet cross-linker UVP source.

## 2.4 Microfluidic Chip

Passive (pump-free) liquid flow and sweat storage was achieved using a PMMA based microfluidic chip (Fig. 3) incorporating the highly adsorbent material and cotton thread. The multilayer system (Fig. 4) was made up using PSA and PMMA layers cut with a  $\text{CO}_2$ -laser ablation system. The PMMA base (1, Fig. 4) contained the inlet hole (for fluid transfer from the 3D-printed sweat harvesting baseplate). An 86  $\mu\text{m}$  thick PSA layer was used to attach a 500  $\mu\text{m}$  thick PMMA (2, Fig. 4), cut to provide channels and location for the adsorbent material.

The absorbent material (pre-washed with deionised water to remove any surfactant or ionic impurities, and dried at 65  $^\circ\text{C}$ ) was laser cut in two patterns, the electrode and channel configuration (to cover the electrodes and



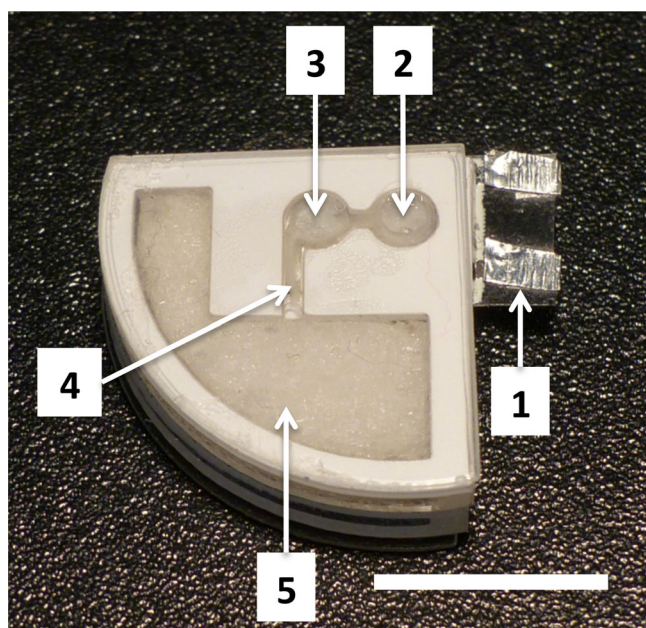


Fig. 3. Electrode locations and fluidic system. The electrodes connect to the Shimmer electronics board through silver tape connections (1). The sweat passes from the skin through a short vertical channel to the ISE (2) and passes laterally to the reference electrode (3) (both the ISE and reference electrodes are ca. 3 mm diameter with a 500  $\mu\text{m}$  height above giving a volume of 3.53  $\mu\text{l}$  over each), and through a short connecting channel (4) to the high capacity absorbent material (5) for sample storage (total storage volume of 344  $\mu\text{l}$ ). Fluidic movement is driven by capillary action; i.e. no pump is required. Variation of the width of the connecting fluidic channel (4) enables the overall flow rate of the system to be modulated. Scale bar = 1 cm

fill the channels) and the configuration of the sample collection reservoir (5, Fig. 3), which is easily removed for subsequent quantification of the total amount of sweat gathered during trials, and for analysis of the aggregated sweat sample using reference methods. A layer of 86  $\mu\text{m}$  PSA was used to attach both the electrochemical-sensing chip (3, Fig. 4) and the 3 mm PMMA sample reservoir en-

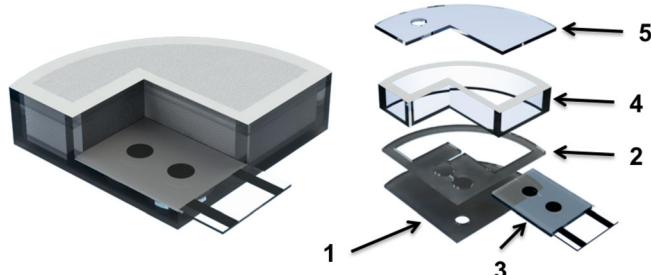


Fig. 4. CAD images of fluidic chip and electrodes, left, and its individual components, right, consisting of (1) 500  $\mu\text{m}$  PMMA base and inlet layer, (2) 500  $\mu\text{m}$  PMMA layer with channels with identical PSA on both sides for adhesion to adjacent layers including (3) the electrochemical sensor and (4) 3 mm PMMA layer to house the absorbent material. The device is sealed by (5) 500  $\mu\text{m}$  PMMA vented lid bonded to the device with PSA.

closure (4, Fig. 4). A 86  $\mu\text{m}$  PSA layer attached the final 500  $\mu\text{m}$  PMMA (5, Fig. 4) enclosing layer.

Control over the flow rate through the channel was achieved by adjusting the width of the connecting channel (Fig. 3, (4)). Microfluidic chips were fabricated with 250  $\mu\text{m}$ , 500  $\mu\text{m}$  and 750  $\mu\text{m}$  channel widths, and incorporated into prototype platforms for fluid transfer testing. Each prototype was placed in contact with deionized water, and the mass of water transferred through the fluidic system measured every 30 s.

## 2.5 Data Collection, Processing and Communication

The prototype platforms incorporate a custom-designed electronics board provided by Shimmer for accurate measurement of the ISE-RE potential (Fig. 5). The board incorporates high impedance inputs necessary for ISE monitoring and a Bluetooth module for wireless communication with a desktop or laptop computer, smart phone or tablet. Along with the Shimmer hardware, an application program interface (API) for Matlab was created which allowed the results to be visualised and processed remotely.

The Li-polymer battery provides enough power to maintain the platform in continuous use for up to 3 hours. This will be extended significantly through optimization of the platform operation during scaled-up trials planned for the coming months.

## 2.6 Real-time On-body Sweat Sodium Monitoring Trials

Healthy male athletes with moderate to high fitness levels participated in indoor exercise trials using stationary cycles (average room temperature of 25  $^{\circ}\text{C}$ ) and a cycle ergometer (Monark Exercise, Sweden) at an intensity load high enough to induce sweating. The sampling area was cleaned prior to positioning the prototype platforms on the upper arm. The 'pod' type platform was located on the upper arm and held in position using elastic straps incorporating Velcro for easy adjustment.

All experiments involving human subjects were performed in compliance with Irish Law and Institutional Guidelines, see <https://www4.dcu.ie/researchsupport/research-ethics/guidelines.shtml>, and were approved by

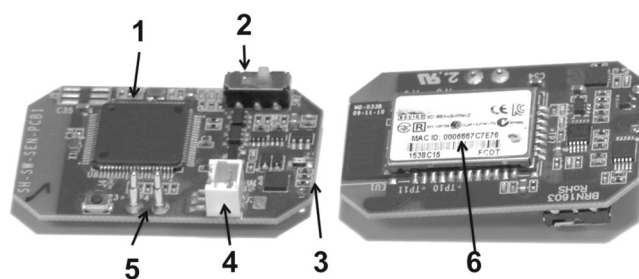


Fig. 5. Top (left) and bottom (right) views of the custom-designed electronics. 1: MSP 430 microcontroller (Texas Instruments); 2: power switch; 3: battery connections; 4: molex sensor connections; 5: battery charging pins; and 6: bluetooth module.

DCU Research Ethics Committee. Informed consent was obtained for all experiments involving human subjects. Trials lasted from 15 to 30 min.

## 2.7 Other Instrumentation

During electrochemical optimization and initial on-bench testing potentiometric measurements were recorded using a high impedance multi-channel voltammeter (MCV) from Lawson Labs (USA), along with a double-junction Ag/AgCl reference electrode (Sigma-Aldrich, Dublin). Electropolymerisation was achieved using a CHI760d potentiostat (CH-instruments, USA). Photo-polymerisation of the acrylate monomers (i.e. for the realisation of reference electrodes) was obtained using the CL-1000 ultraviolet cross-linker UVP. The CO<sub>2</sub> laser ablation system was an Epilog Zing Laser Engraver (Epilog, USA) whereas the thermal roller laminator (Titan-110) was from GBC Films (USA). A Stratasys Objet260 Connex1 3D printer was used to print the casings and enclosures for the prototype platforms.

## 3 Results and Discussion

### 3.1 Na<sup>+</sup> Sensor Sensitivity

The response characteristics of the Na<sup>+</sup> ISEs were initially characterized using the Lawson Lab MCV. Responses to NaCl concentrations from 10<sup>-4</sup> to 10<sup>-1</sup> M were analysed in single decade intervals. The overall response was slightly sub-Nernstian ( $R^2 > 0.99$ ), with an average slope of  $58.03 \pm 3.458$  mV/decade Na<sup>+</sup> (Fig. 6,  $n=4$ ). The solid-state REs had an average slope of  $-1.337 \pm 1.468$  mV/decade ( $n=4$ ) over the same range.

### 3.2 Fluidic System

Fluid transport through the fluidic system is driven by capillary forces arising in the absorbent material which

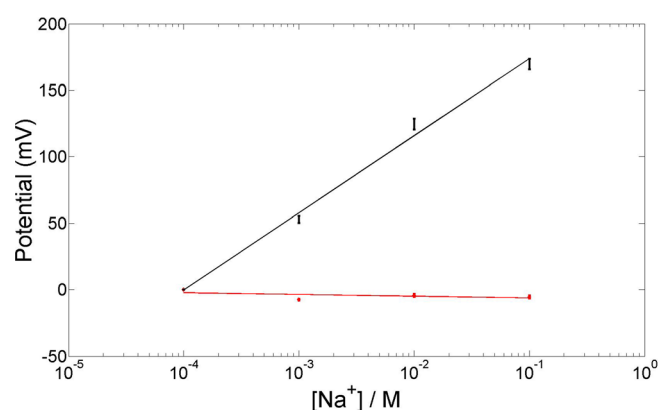


Fig. 6. Average response of ISEs (black) and reference electrodes (red) to changes in Na<sup>+</sup> concentration from 10<sup>-4</sup> to 10<sup>-1</sup> M measured using the MCV benchtop reference instrument. ISEs: slope =  $58.003 (\pm 3.458, n=4)$  mV/decade and REs: slope =  $-1.337 (\pm 1.468, n=4)$  mV/decade.

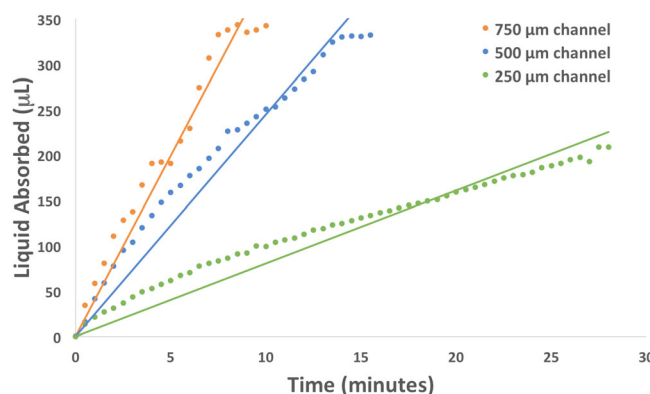


Fig. 7. Modulation of platform flow rate by varying the width of the connecting fluidic channel (4) in Fig. 3. The average flow-rates of each channel over the period of the experiments were  $38.20 \mu\text{L}/\text{min} \pm 1.34$  for the 750  $\mu\text{m}$  channel,  $21.48 \mu\text{L}/\text{min} \pm 0.57$  for the 500  $\mu\text{m}$  channel and  $6.61 \mu\text{L}/\text{min} \pm 0.11$  for the 250  $\mu\text{m}$  channel ( $n=3$  replicates in all cases). For the 750  $\mu\text{m}$  and 500  $\mu\text{m}$  channels, the volume absorbed falls off around 330  $\mu\text{L}$  which is consistent with saturation of the platform storage volume.

pulls sample from the skin past the electrodes and into the sample collection area. The absorbent material is a three layer composite made up of an adsorbent cellulose layer between two abrasive resistant polypropylene layers. The flow rate of the sample delivery over the electrodes was varied by changing the width dimension of the connecting channel (4, Fig. 3) from 750 to 500 and 250  $\mu\text{m}$ . Using these, we obtained flow rates of 38.20, 21.48 and 6.61  $\mu\text{L}/\text{min}$ , respectively, Fig. 7. These results show that the sweat flow rate through the device can be controlled through applying a constriction within the fluidic system. The flow rate obtained is reasonably linear for all three channel widths throughout the durations of the experiments.

### 3.3 On-body Trials

Calibrations (Fig. 8) of the combined solid-state ISE-RE pairs integrated within the prototype platform were performed using 10<sup>-4</sup> to 10<sup>-1</sup> M NaCl standard solutions, prior to commencing on-body trials. The solutions were pipetted through the inlet onto the absorbent material which wicked the liquid across the electrodes to the sample collection reservoir. The total volume from inlet to entry to sample collection area (with the 500  $\mu\text{m}$  channel used in the trials) was 10.28  $\mu\text{L}$  meaning slightly more than 10  $\mu\text{L}$  of sample should be sufficient to entirely displace the preceding solution. The platforms were pre-primed before use with 10<sup>-4</sup> M NaCl by injecting enough volume to provide full contact with the electrodes and establish a stable baseline that would enable arrival of the more concentrated sweat to be observed through a rapid increase in the signal.

The SWEATCH prototype (pod design, Fig. 9) was positioned on a volunteer's arm before commencing to

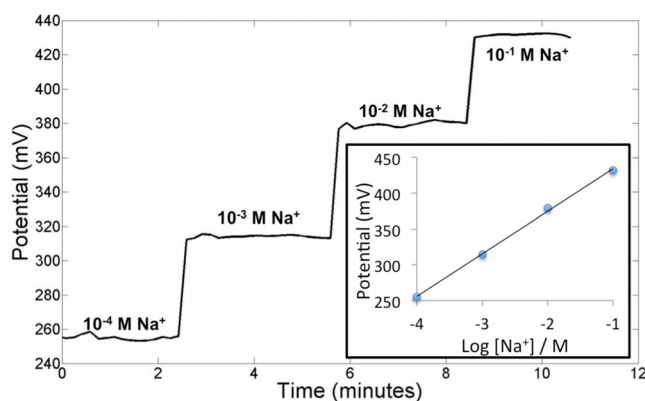


Fig. 8. Calibration of a  $\text{Na}^+$ -ISE and RE output signal using the Shimmer board, giving a slope of 56.98 mV and an  $R^2$  value of 0.99.



Fig. 9. SWEATCH device in place on volunteer's arm during a trial on a stationary exercise bicycle.

a period of exercise on a stationary bicycle. Prior to positioning the device, the sampling location was cleaned with a sterile wipe. The volunteer continued to exercise while the output signal of the platform was recorded wirelessly in real-time, (Fig. 10). After approximately 4 min the signal began to increase rapidly indicating the arrival of the initial sweat at the electrodes.

Thereafter, a steady increase in signal was observed until approximately 10 min at which point the signal stabilised until the end of the trial after 15 min.

#### 4 Discussion

Despite recent advances and increasing focus by industry and academic research teams, gathering personalised biochemical information in real time remains very challenging, as outlined in the introduction. The two designs we have investigated have the same contributing components (sampling baseplate, fluidic system, electrochemical sensors, sample storage and capillary driven movement, elec-

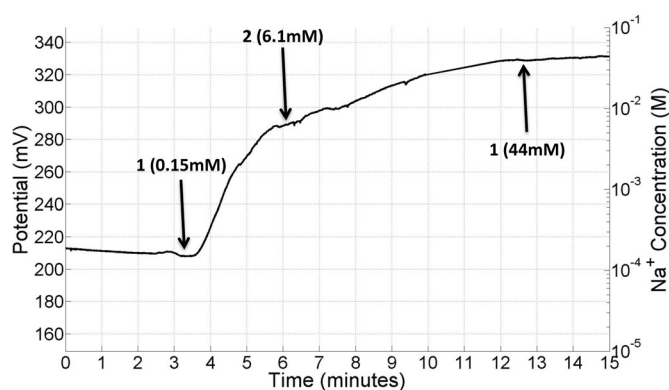


Fig. 10. Real-time data obtained during a trial. The initial signal up to (1) reflects the  $10^{-4}$  M NaCl conditioning solution which is initially in contact with the electrodes. After ca. 4 minutes, sweat reaches the electrodes, which results in a rapid increase in the signal. By point (2), the residual conditioning solution has been washed away from the electrodes and the signal is now representative of the sweat. From (2) to (3) the signal increases gradually to a steady state equivalent to ca. 44 mM  $\text{Na}^+$ .

tronics and power) albeit with pros and cons associated with the designs. For example, the watch-design is more compact and less intrusive for the wearer, while the pod-design enables the electronics and fluidics components to be physically separated, and allows for larger sample storage volumes (and therefore use periods) due to the increased footprint. The pod design was used in the trial as shown in Fig. 9.

Near-Nernstian calibration slopes were obtained from the solid-state ISE-RE combination using both the MCV bench (Fig. 6) and Shimmer board (Fig. 8), with excellent correlation between the two measurement systems, suggesting that the electrodes and the Shimmer customized electronics board were functioning satisfactorily. The interconnecting channel width (Fig. 3) was found to have a significant influence on the overall flow rate of fluid through the platforms, with the flow rate decreasing as the channel was increasingly constricted (Fig. 7). The results obtained are an indication of the maximum flow rates that can be expected through the system, as the fluidic source volume was not restricted in these experiments. For best results on-body, the flow rate through the platform should be greater than the local maximum skin sweat rate, to ensure that the locally generated sweat is effectively transferred into the device, and does not build up. As previously reported by Smith et al. [21], the skin sweat rate varies according to multiple factors, including body location, intensity of the exercise, and the person exercising. Therefore, an adjustable sampling flow rate could be a very useful feature (e.g. using a calibrated screw), as it allows the overall sampling time and sweat uptake rate to be tuned according to the above variables.

The results from on-body trials indicate that transfer of sweat from the skin to the electrodes is quite efficient, manifesting as the rapid rise in the signal commencing around 4 min (Fig. 10). After this trial, the amount of



sweat recovered from the adsorbent material was 87.45 mg. Allowing for the fluidic system dead-volume (10.28  $\mu\text{L}$ ) and assuming a density of 1 mg/ $\mu\text{L}$ , the total amount of sweat gathered was ca. 100  $\mu\text{L}$ . It is difficult to say exactly when the sweat began to flow through the fluidic system during the initial 4 min period, but, assuming it was flowing for the entire 15 minute period, we can estimate the average sweat flow rate to be in the region of 6–7  $\mu\text{L}/\text{min}$ . The fluidic system used in this study had a connector channel width of 500  $\mu\text{m}$ , which from Fig. 4 should be able to sample up to 21.48  $\mu\text{L}/\text{min}$ . Hence we can conclude that the device maximum flow rate was well in excess of the sweat flow rate in the trial.

From comparisons with the pre-trial and post-trial calibrations, the steady-state potential of ca. 330 mV is equivalent to a sodium concentration of ca. 44 mM, which is consistent with concentrations we [3] and others [11] have found in related studies. Interestingly, a recent analysis by Traeger et al. of 13,785 sweat tests performed over a period of 23 years found a mean sodium concentration of  $33.8 \pm 15.7$  mM of 204 Cystic Fibrosis negative patients over the age of 18 years [22]. Comparison with preliminary data from other trials performed suggest a range of 7 mM–44 mM but a more extensive study is in progress to investigate this further.

## 5 Conclusions

In this paper, we have demonstrated a wearable prototype platform that can;

- Harvest sweat from a pre-selected location on the body during exercise trials;
- Transport the sweat from the skin to electrodes that measure the  $\text{Na}^+$  concentration in the sweat;
- Further transport the sweat to an in-device storage area for subsequent analysis post-trial;
- Make the measured data available in real-time using Bluetooth wireless connectivity

These platforms can be developed further to incorporate detection for a range of relevant analytes such as  $\text{K}^+$  and other relevant analytes. In addition, the sampling flow rate through the device can be varied by constricting the channel width. In this paper, we present very preliminary results from a single limited trial. We are currently fabricating batches of these platforms for further characterization and use in scaled up trials that should enable a clearer picture of how the  $\text{Na}^+$  concentration in sweat varies during exercise trials to emerge.

## Acknowledgements

We acknowledge financial support from Science Foundation Ireland (SFI) under the Insight Centre award, Grant Number SFI/12/RC/2289, the European Union Marie Curie International Fellowships grant 'MASK', Project no: 269302, and the Australian Research Council Centre

of Excellence Scheme (Project Number CE 140100012). The authors would also like to thank the Australian National Nanofabrication Facility – Materials node for equipment use.

## References

- [1] G. Matzeu, L. Florea, D. Diamond, *Sens. Actuators B Chem.* **2015**, *211*, 403–418.
- [2] H. Garrett DeYoung, *High Technol.* **1983**, 41–49.
- [3] B. Schazmann, D. Morris, C. Slater, S. Beirne, C. Fay, R. Reuveny, N. Moyna, D. Diamond, *Anal. Methods* **2010**, *2*, 342–348.
- [4] A. J. Bandodkar, D. Molinnus, O. Mirza, T. Guinovart, J. R. Windmiller, G. Valdés-Ramírez, F. J. Andrade, M. J. Schöning, J. Wang, *Biosens. Bioelectron.* **2014**, *54*, 603–609.
- [5] J. Kim, G. Valdés-Ramírez, A. J. Bandodkar, W. Jia, A. G. Martinez, J. Ramírez, P. Mercier, J. Wang, *The Analyst* **2014**, *139*, 1632.
- [6] H. Yao, A. J. Shum, M. Cowan, I. Lähdesmäki, B. A. Parviz, *Biosens. Bioelectron.* **2011**, *26*, 3290–3296.
- [7] “Smart contact lenses move closer to reality: Novartis and Google announce partnership to develop the new glucose-sensing technology,” can be found under <http://diatribe.org/issues/65/new-now-next/11>, **2014**.
- [8] Y. S. Rim, S.-H. Bae, H. Chen, J. L. Yang, J. Kim, A. M. Andrews, P. S. Weiss, Y. Yang, H.-R. Tseng, *ACS Nano* **2015**, *9*, 12174–12181.
- [9] A. Lynch, D. Diamond, M. Leader, *The Analyst* **2000**, *125*, 2264–2267.
- [10] B. Chua, S. P. Desai, M. J. Tierney, J. A. Tamada, A. N. Jina, *Sens. Actuators Phys.* **2013**, *203*, 373–381.
- [11] W. Gao, S. Emaminejad, H. Y. Y. Nyein, S. Challa, K. Chen, A. Peck, H. M. Fahad, H. Ota, H. Shiraki, D. Kiriya, et al., *Nature* **2016**, *529*, 509–514.
- [12] Adam Brown, Kelly Close, “Abbott’s FreeStyle Libre – Transforming Glucose Monitoring Through Utter Simplicity, Fingersticks Aside!,” can be found under <http://diatribe.org/abbott-freestyle-libre-transforming-glucose-monitoring-through-utter-simplicity-fingersticks>, **2015**.
- [13] X. Huang, Y. Liu, K. Chen, W.-J. Shin, C.-J. Lu, G.-W. Kong, D. Patnaik, S.-H. Lee, J. F. Cortes, J. A. Rogers, *Small* **2014**, *10*, 3083–3090.
- [14] A. J. Bandodkar, J. Wang, *Trends Biotechnol.* **2014**, *32*, 363–371.
- [15] M. H. Rosner, J. Kirven, *Clin. J. Am. Soc. Nephrol.* **2006**, *2*, 151–161.
- [16] A. S. Verkman, L. J. V. Galletta, *Nat. Rev. Drug Discov.* **2009**, *8*, 153–171.
- [17] D. Diamond, G. Svehla, E. Seward, M. McKervery, *Anal. Chim. Acta* **1988**, *204*, 223–231.
- [18] C. Zuliani, G. Matzeu, D. Diamond, *Electrochimica Acta* **2014**, *132*, 292–296.
- [19] J. Hu, A. Stein, P. Bühlmann, *TrAC Trends Anal. Chem.* **2016**, *76*, 102–114.
- [20] G. Matzeu, C. O’Quigley, E. McNamara, C. Zuliani, C. Fay, T. Glennon, D. Diamond, *Anal. Methods* **2016**, *8*, 64–71.
- [21] C. J. Smith, G. Havenith, *Eur. J. Appl. Physiol.* **2011**, *111*, 1391–1404.
- [22] N. Traeger, Q. Shi, A. J. Dozor, *J. Cyst. Fibros.* **2014**, *13*, 10–14.

Received: February 22, 2016

Accepted: March 15, 2016

Published online: ■ ■ ■ ■, 0000

## FULL PAPERS

*T. Glennon, C. O'Quigley,  
M. McCaul, G. Matzeu, S. Beirne,  
G. G. Wallace, F. Stroeescu,  
N. O'Mahoney, P. White,  
D. Diamond\**



**'SWEATCH': A Wearable Platform  
for Harvesting and Analysing Sweat  
Sodium Content**

